Subcellular localization of NAPE-PLD and DAGL-α in the ventromedial nucleus of the hypothalamus by a preembedding immunogold method

ARTICLE *in* HISTOCHEMIE · APRIL 2014

Impact Factor: 3.05 · DOI: 10.1007/s00418-013-1174-x · Source: PubMed

Histochem Cell Biol
DOI 10.1007/s00418-013-1174-x

ORIGINAL PAPER

Subcellular localization of NAPE-PLD and DAGL-α in the ventromedial nucleus of the hypothalamus by a preembedding immunogold method

Leire Reguero · Nagore Puente · Izaskun Elezgarai · Almudena Ramos-Uriarte · Inmaculada Gerrikagoitia · José-Luis Bueno-López · Francisco Doñate · Pedro Grandes

Accepted: 5 December 2013

Abstract The hypothalamus and the endocannabinoid system are important players in the regulation of energy homeostasis. In a previous study, we described the ultrastructural distribution of CB_1 receptors in GABAergic and glutamatergic synaptic terminals of the dorsomedial region of the ventromedial nucleus of the hypothalamus (VMH). However, the specific localization of the enzymes responsible for the synthesis of the two main endocannabinoids in the hypothalamus is not known. The objective of this study was to investigate the precise subcellular distribution of *N*-arachidonoylphospatidylethanolamine phospholipase D (NAPE-PLD) and diacylglycerol lipase α (DAGL-α) in the dorsomedial VMH of wild-type mice by a high resolution immunogold electron microscopy technique. Knock-out mice for each enzyme were used to validate the specificity of the antibodies. NAPE-PLD was localized presynaptically and postsynaptically but showed a preferential distribution in dendrites. DAGL-α was mostly postsynaptic in dendrites and dendritic spines. These anatomical results contribute to a better understanding of the endocannabinoid modulation in the VMH nucleus. Furthermore, they support the idea that the dorsomedial VMH displays the necessary machinery for the endocannabinoid-mediated modulation of synaptic transmission of brain circuitries that regulate important hypothalamic functions such as feeding behaviors.

L. Reguero · N. Puente · I. Elezgarai · A. Ramos-Uriarte · I. Gerrikagoitia · J.-L. Bueno-López · F. Doñate · P. Grandes (✉)
Department of Neurosciences, Faculty of Medicine and Dentistry, University of the Basque Country UPV/EHU, 48940 Leioa, Vizcaya, Spain
e-mail: pedro.grandes@ehu.es

Keywords Endocannabinoids · Synthesizing enzymes · Energy homeostasis · Immunocytochemistry · Electron microscopy

Introduction

The hypothalamus plays a crucial role in the regulation of energy balance and food intake (Berthoud 2002). In particular, the hypothalamic ventromedial nucleus (VMH) participates in several homeostatic and behavioral functions, including the regulation of appetite and energy balance (McClellan et al. 2006; Kim et al. 2008). This nucleus has also been proposed as a satiety hub possibly due to its strong excitatory input to proopiomelanocortin (POMC) arcuate neurons leading to the activation of anorexigenic neuronal pathways (Sternson et al. 2005).

Derivatives of the plant *Cannabis sativa* regulate food intake, and the endocannabinoid system controls neuronal signaling of hypothalamic pathways (Pagotto et al. 2006). The endocannabinoid system is a complex endogenous signaling system that participates in multiple metabolic pathways (Cota and Woods 2005). It is composed of cannabinoid receptors, their endogenous ligands or endocannabinoids and the proteins involved in their synthesis and degradation, as well as the intracellular signaling pathways regulated by endocannabinoids (De Petrocellis et al. 2004). The two main endocannabinoids are *N*-arachidonoylethanolamine or anandamide (Devane et al. 1992) and 2-arachidonoylglycerol (2-AG) (Mechoulam et al. 1995; Sugiura et al. 1995). The levels of both endocannabinoids in the hypothalamus increase during fasting and decrease following food intake reaching a critical point that favors a motivational state for food intake (Kirkham et al. 2002; Di Marzo and Matias 2005; Pagotto et al. 2006; Matias

Published online: 18 December 2013

and Di Marzo 2007). Actually, anandamide administration into the VMH stimulates appetite in rats (Jamshidi and Taylor 2001), while animals chronically treated with CB_1 antagonists (Colombo et al. 1998; Di Marzo et al. 2001; Pagotto et al. 2006) and CB_1-KO mice (Di Marzo et al. 2001; Cota et al. 2003; Pagotto et al. 2006) exhibit an anorexigenic phenotype. Moreover, activation of CB_1 receptors at GABAergic synapses in the ventral striatum has a hypophagic effect while brain CB_1 receptors at glutamatergic synapses are responsible of the cannabinoids-mediated increase in food intake (Bellocchio et al. 2010). In view of the described observations, we hypothesized that the main components of the endocannabinoid system, such as CB_1 receptors and the synthesizing enzymes for the two principal endocannabinoids, may be at neural circuits that converge into the ventromedial nucleus of the hypothalamus. We have previously shown with immunoelectron microscopy that a similar proportion (~25 %) of symmetric (inhibitory) and asymmetric (excitatory) synaptic terminals localizes CB_1 receptors in the dorsomedial region of the VMH (Reguero et al. 2011).

As to the synthesizing enzymes, *N*-arachidonoylphospatidylethanolamine phospholipase D (NAPE-PLD) is the main responsible for the synthesis of anandamide, while 2-AG is synthesized by a diacylglycerol lipase (DAGL-α) (Basavarajappa 2007). The localization of these enzymes has been previously described in neurons and glia in several regions of the central nervous system (CNS) such as the hippocampus, cerebellum, amygdala, striatum, neocortex, spinal cord or circumventricular areas (Egertová et al. 1998, 2003, 2008; Gulyas et al. 2004; Katona et al. 2006; Yoshida et al. 2006, 2011; Uchigashima et al. 2007, 2011; Cristino et al. 2008; Nyilas et al. 2008; Suárez et al. 2010; Hegyi et al. 2012; Tanimura et al. 2012). However, their specific distribution in the hypothalamus has not been characterized yet.

The aim of this study was to analyze the precise anatomical localization of NAPE-PLD and DAGL-α in the mouse dorsomedial VMH. For this purpose, specific antibodies for each enzyme applied to the VMH of wild-type and knock-out mice were combined with a high resolution preembedding immunocytochemical method for electron microscopy.

Experimental procedures

Animal treatment

The procedures were carried out in accordance with European Communities Council Directives (2003/65/CE and 2010/63/UE) and current Spanish regulations (Real Decreto 53/2013 and Ley 32/2007). The protocols for animal care and use were approved by the appropriate Committee at the University of the Basque Country UPV/EHU (CEBA/93/2010/GRANDESMORENO). Furthermore, great efforts were made in order to minimize the number and suffering of the animals used.

Six wild-type C57BL/6 N female mice (3–5 month old) were used in this study. Animals were maintained under standard conditions (12 h light/dark cycle) with food (standard chow, Global Diet 2014S, Harlan) and water ad libitum. Mice were deeply anesthetized at a timepoint comprised between 10.00 and 12.00 am by intraperitoneal injection of ketamine/xilacine (80/10 mg/kg body weight) and were transcardially perfused at room temperature (RT, 20–25 °C) with phosphate-buffered saline (PBS 0.1 M, pH 7.4) for 20 s, followed by the fixative solution made up of 4 % formaldehyde (freshly depolymerized from paraformaldehyde), 0.2 % picric acid and 0.1 % glutaraldehyde in phosphate buffer (PB 0.1 M, pH 7.4) for 10–15 min. Then, brains were removed from the skull and postfixed in the fixative solution for approximately 1 week at 4 °C. Afterward, they were stored at 4 °C in 1:10 diluted fixative solution until used. Furthermore, tissue from NAPE-PLD–KO mice (perfused with 4 % formaldehyde and sliced at 30 μm with a cryotome) was generously provided by Dr. Juan Suárez (Laboratorio de Medicina Regenerativa, IBIMA-Hospital Carlos Haya, Málaga, Spain). The gene disruption construct was generated using PCR-amplified 5′ and 3′ homologous recombination fragments surrounding exon 4 of the NAPE-PLD gene. Chimeric mice on a C57BL/6 background were generated. These mice were second or third generation offspring from intercrosses of 129SvJ-C57BL/6 PLD ± mice (Leung et al. 2006). Moreover, tissue from DAGL-α–KO mouse (perfused with 4 % formaldehyde) was generously gifted by Dr. Masahiko Watanabe (Department of Anatomy, Hokkaido University School of Medicine, Sapporo, Japan). These null mutant mice were developed from a C57BL/6N strain generated by disrupting exon 3 and 4 of DAGL-α gene (Tanimura et al. 2010). Coronal hypothalamic vibrosections were cut at 40 μm and collected in 0.1 M PB at RT.

Specificity controls of the NAPE-PLD antibody: immunoperoxidase method for light microscopy

Specificity of the NAPE-PLD immunostaining was assessed by the positive control in the hippocampus and in hippocampus of NAPE-PLD knock-out mice. For these controls, coronal hippocampal sections obtained from wild-type and NAPE-PLD–KO mice were preincubated in a blocking solution of 10 % bovine serum albumin (BSA), 0.1 % sodium azide and 0.5 % triton X-100 prepared in Tris–HCl-buffered saline (TBS 1X, pH 7.4) for 30 min at RT. Then, they were incubated in a primary polyclonal guinea-pig anti-NAPE-PLD antibody (4 μg/ml, Frontier

Science co. Ltd, Shinko-nishi, Ishikari, Hokkaido, Japan) prepared in the blocking solution, on a shaker for 2 days at 4 °C. After several washes in 1 % BSA and 0.5 % triton X-100 in TBS, tissue sections were incubated in a secondary biotinylated donkey anti-guinea-pig IgG (1:200, Jackson ImmunoResearch Laboratories Inc., Baltimore, PA, USA) prepared in the washing solution for 1 h on a shaker at RT. The brain sections were washed in the washing solution described above and processed by a conventional avidin–biotin peroxidase complex method (ABC, Elite, Vector Laboratories, Burlingame, CA, USA). Tissue was incubated in the avidin–biotin complex (1:50) prepared in the washing solution for 1 h at RT. Then, sections were washed and incubated with 0.05 % diaminobenzidine in 0.1 M PB with 0.5 % triton-X100 and using 0.01 % hydrogen peroxide as a chromogen, for 5 min at RT. Finally, tissue was mounted, dehydrated in graded alcohols (50°, 70°, 96°, 100°) to xylol and coverslipped with DPX. Sections were observed and photographed with a light microscope Zeiss Axiophot. Figure compositions were made at 600 dots per inch (dpi). Labeling and minor adjustments in contrast and brightness were made using Adobe Photoshop (CS, Adobe Systems, San Jose, CA, USA).

Furthermore, the specificity of the NAPE-PLD antibody has also been confirmed in previous studies (Nyilas et al. 2008; Puente et al. 2011).

Preembedding immunogold method for electron microscopy. Specificity control of the DAGL-α antibody

Sections were preincubated in a blocking solution of 10 % BSA, 0.1 % sodium azide and 0.02 % saponin in TBS for 30 min at RT. Then, they were incubated in the corresponding primary antibody: NAPE-PLD (4 μg/ml, as described above) or DAGL-α (2 μg/ml, made in rabbit, Frontier Science co. Ltd, Shinko-nishi, Ishikari, Hokkaido, Japan) prepared in the blocking solution but with 0.004 % saponin, on a shaker for 2 days at 4 °C. Specificity of the DAGL-α antibody was assessed in hypothalamus of DAGL-α knock-out mice processed for this method. After several washes with 1 % BSA in TBS, tissue sections were incubated in the corresponding (anti-guinea-pig or anti-rabbit) secondary 1.4 nm nanogold antibody (1:100, Fab' fragment, Nanoprobes Inc., Yaphank, NY, USA) prepared in the same solution as the primary antibody for 3 h on a shaker at RT. Then, tissue was washed overnight at 4 °C and postfixed in 1 % glutaraldehyde for 10 min. After several washes in double distilled water, gold particles were silver-intensified with a HQ Silver Kit (Nanoprobes Inc., Yaphank, NY, USA) for 12 min in the dark. Then, tissue was extensively washed in double distilled water and in 0.1 M PB and osmicated in 1 % osmium tetroxide for 20 min. After washing in 0.1 M PB, sections were dehydrated in graded alcohols (50°, 70°, 96°, 100°) to propylene oxide and embedded in Epon resin 812. Eighty-nanometer ultrathin sections were collected on mesh nickel grids, stained with lead citrate for 20 min and examined in a PHILIPS EM208S electron microscope. Tissue preparations were photographed by using a digital camera coupled to the electron microscope. Figure compositions were made at 600 dots per inch (dpi). Labeling and minor adjustments in contrast and brightness were made using Adobe Photoshop (CS, Adobe Systems, San Jose, CA, USA).

The specificity of the DAGL-α antibody has also been confirmed in previous studies (Yoshida et al. 2006; Uchigashima et al. 2007; Puente et al. 2011).

Statistical analysis

Electron micrographs (18,000–28,000X) were taken from grids containing silver-intensified gold particles in hypothalamic 80 nm ultrathin sections. All of them showed a similar labeling intensity indicating that selected areas were at the same depth. Furthermore, to avoid false negatives, only ultrathin sections in the first 1.5 μm from the surface of the tissue block were examined.

For subcellular localization of DAGL-α, positive labeling was considered if at least 1 immunoparticle was within approximately 30 nm from the plasmalemma. On the other hand, positive labeling for NAPE-PLD was considered if at least 1 immunoparticle was within approximately 30 nm from the plasmalemma or inside the profile. Immunopositive and immunonegative synaptic profiles (dendrites or terminals) were identified and counted. Then, the percentage of immunolabeled profiles for each protein was calculated and displayed as mean ± SEM using a statistical software package (GraphPad Prism 4, GraphPad Software Inc, San Diego, USA). Group differences were compared by chi-square test, $p < 0.05$. Also, silver-intensified gold particles were counted, and semiquantification of the immunogold labeling on total synaptic profiles was performed. Image-J software (1.43u version, NIH, USA) was used to measure membrane length and analyzed area. Finally, density of immunoparticles (immunoparticles/μm membrane length for DAGL-α and immunoparticles/μm^2 for NAPE-PLD) was determined.

Results

Specificity controls for NAPE-PLD and DAGL-α

We investigated NAPE-PLD immunostaining in the hippocampal dentate gyrus of NAPE-PLD–WT (Fig. 1a, a′) and NAPE-PLD–KO mice (Fig. 1b, b′) by the immunoperoxidase method for light microscopy. We observed in the WT the typical dense NAPE-PLD immunostaining in the hilus of the dentate gyrus that it was absence in

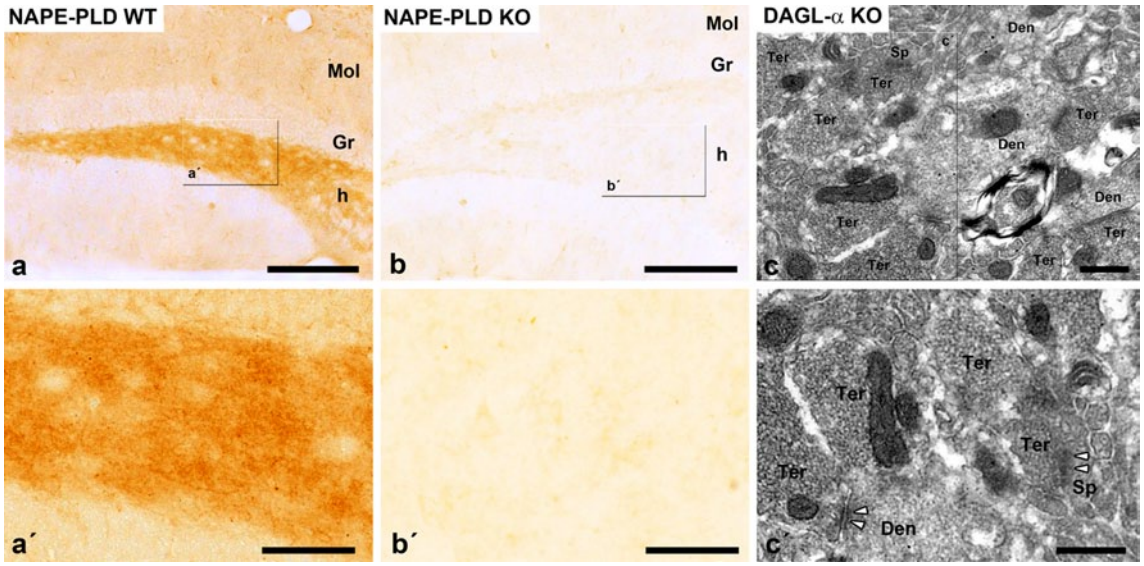

Fig. 1 Specificity controls of the antibodies. **a**, **b** Control of NAPE-PLD immunostaining in the layers of fascia dentate (*Mol* molecular; *Gr* granular; *h* hilus) of NAPE-PLD–WT and NAPE-PLD–KO mice. Preembedding immunoperoxidase method for light microscopy. *Frames* in **a** and **b** are shown at higher magnification in **a′** and **b′**, respectively. The strong immunostaining observed in the hilus of WT is abolished in the KO tissue, indicating the specificity of the antibody used. *Scale bars* 200 μm (**a**, **b**) and 50 μm (**a′**, **b′**). **c** Specificity control of DAGL-α in the dorsomedial VMH of DAGL-α–KO mouse. Preembedding silver-intensified immunogold method for electron microscopy. *Frame* in **c** is shown magnified in **c′**. No immunoparticles are at postsynaptic dendrites (Den) or dentritic spines (Sp) receiving synapses (*arrowheads*) from terminal (Ter) boutons. *Scale bars* 0.5 μm

NAPE-PLD–KO, corroborating the specificity of this antibody. With regard to DAGL-α, we analyzed the dorsomedial VMH region of DAGL-α–KO mice (Fig. 1c, c′) by the preembedding immunogold method for electron microscopy. In this case, we observed no specific immunolabeling, in contrast to the WT shown in Fig. 3.

Immunolocalization of NAPE-PLD in the dorsomedial VMH

First, we analyzed the ultrastructural localization of NAPE-PLD in the dorsomedial region of the VMH using a preembedding immunogold method for electron microscopy (Fig. 2). NAPE-PLD immunoparticles were distributed both at postsynaptic and at presynaptic sites next to the membranes of dendrites and synaptic terminals, respectively (Fig. 2a, b, d, e). Also, NAPE-PLD labeling was observed inside the neuronal profiles (Fig. 2f), frequently associated with intracellular organelles such as the smooth endoplasmic reticulum (Fig. 2c). Furthermore, 45.2 % of the immunoparticles were distributed in dendrites and 41.5 % in synaptic terminals. Also, the proportion of NAPE-PLD immunopositive dendrites was significantly higher (49.5 %) than of the positive terminals (30.9 %, $\chi^2 = 13.71$, $p = 0.0002$) (Fig. 2g). On the contrary, the labeling density measured as immunoparticles/μm^2 was higher in synaptic terminals (3.0 immunoparticles/μm^2) than in dendritic profiles (1.9 immunoparticles/μm^2).

Immunolocalization of DAGL-α in the dorsomedial VMH

Next, we analyzed the ultrastructural localization of the synthesizing enzyme of 2-AG in the dorsomedial region of the mouse VMH by using the same immunoelectron technique. DAGL-α typically showed a postsynaptic localization on membranes of dendrites (Fig. 3a–c) and dendritic spines (Fig. 3d, e). The proportion of postsynaptic DAGL-α immunoparticles corroborated the preferential distribution of DAGL-α in dendrites. Moreover, 54.4 % of dendrites and 44.4 % of dendritic spines are DAGL-α immunopositive (Fig. 3f) (differences not statistically significant $\chi^2 = 2.220$, $p = 0.1363$). Finally, immunolabeling density was estimated between 0.57 immunoparticles/μm in dendrites and 1.02 immunoparticles/μm in dendritic spines.

Discussion

Ultrastructural localization of NAPE-PLD in the dorsomedial VMH

In spite of the great scientific interest on the field of the cannabinoid system, there are only very few studies in the literature about the ultrastructural localization of NAPE-PLD in the brain (Nyilas et al. 2008; Puente et al. 2011). The present investigation is the first evidence on the subcellular distribution of NAPE-PLD in the VMH. Our results

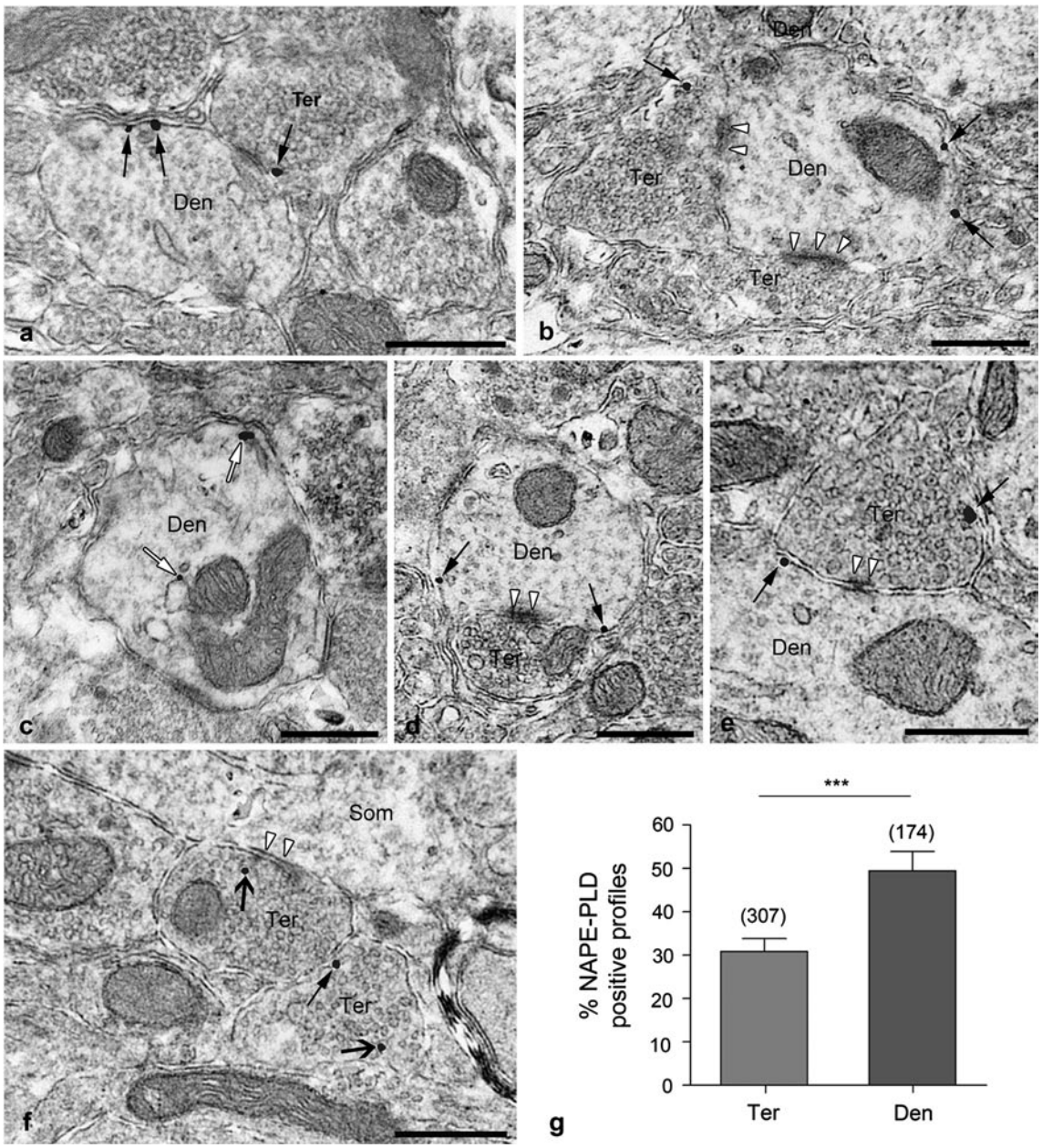

Fig. 2 Ultrastructural localization of NAPE-PLD in the mouse dorsomedial VMH. Preembedding silver-intensified immunogold method for electron microscopy. **a**–**f** NAPE-PLD immunoparticles (*arrows*) are in postsynaptic and presynaptic profiles associated with the membranes (*black close arrows*) of dendrites (Den) and synaptic terminals (Ter), respectively, as well as inside both neuronal compartments (*black open arrows*). Note in **b**, **e** that a presynaptic bouton and a postsynaptic dendrite synaptically contacted (*white arrowheads*) are both NAPE-PLD immunopositive. Observe in **f** a positive terminal making a synapse onto a soma (Som). NAPE-PLD is also associated with intracellular reservoirs like the smooth endoplasmic reticulum (*white close arrows*), as it can be appreciated in detail in **c**. *Scale bars* 0.5 μm. **g** The percentage of immunopositive dendrites (49.5 ± 4.5 %) is significantly higher than the percentage of positive terminals (30.9 ± 2.9 %, $\chi^2 = 13.71$, $p = 0.0002$). Numbers between parentheses indicate the number of analyzed profiles. Total analyzed area 998 μm^2

show that the localization of NAPE-PLD immunoparticles in the dorsomedial region of the VMH is both presynaptic and postsynaptic, but with a preferential distribution in postsynaptic dendrites.

NAPE-PLD expression in the brain and other organs increases with age (Morishita et al. 2005). In mice, the highest brain levels of NAPE-PLD mRNA were detected in granule cells of the dentate gyrus, followed by hippocampal CA3 pyramidal neurons. Moderate–low levels were found in layers II-III of the neocortex, layer II of piriform cortex, olfactory bulb, granule and Purkinje cells in the cerebellum and thalamic and hypothalamic nuclei, such as the

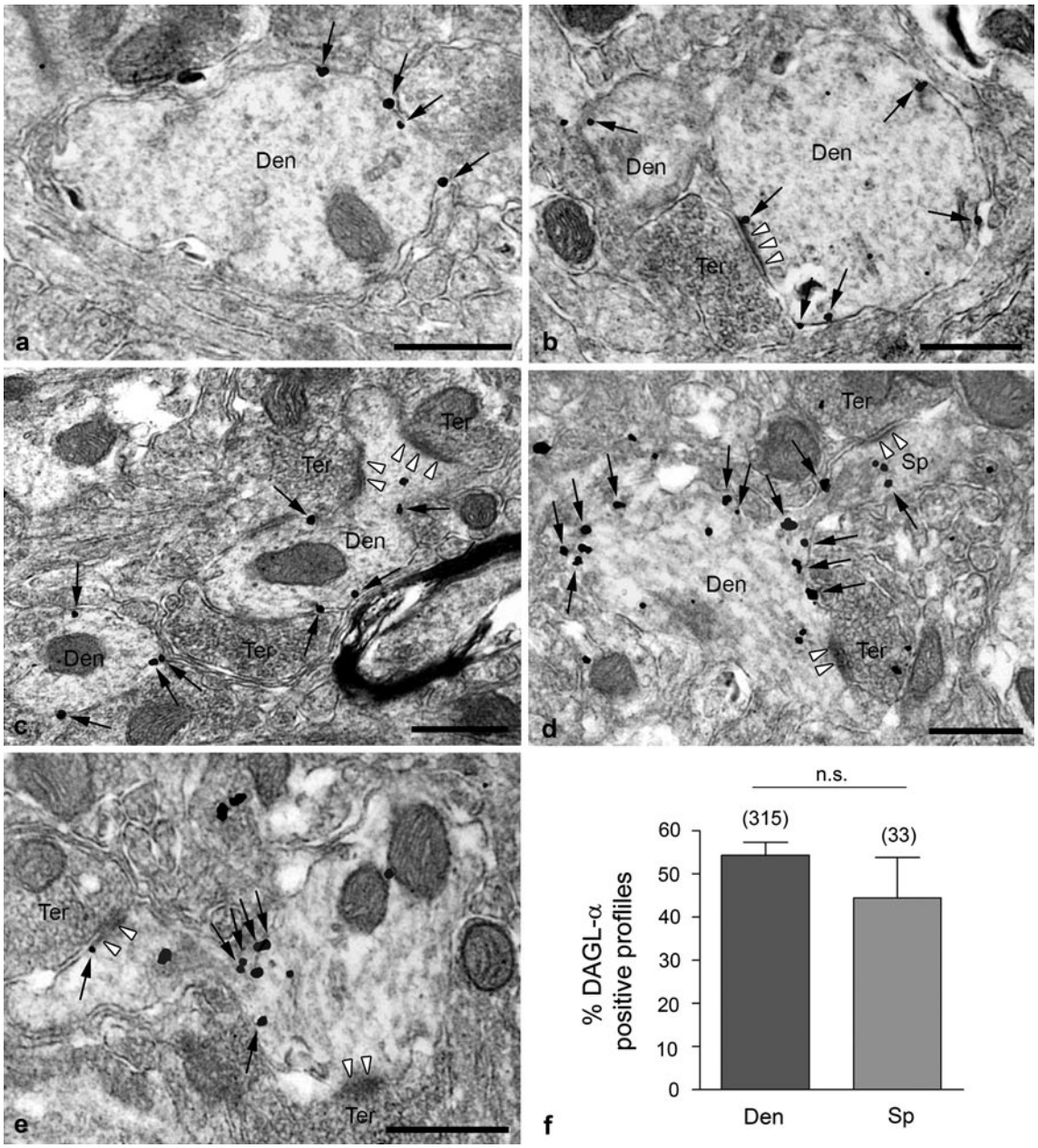

Fig. 3 Ultrastructural localization of DAGL-α in the mouse dorsomedial VMH. Preembedding silver-intensified immunogold method for electron microscopy. **a**–**e** DAGL-α immunoparticles (*black close arrows*) are localized on membranes of dendrites (Den) that receive synaptic contacts (*white arrowheads*) from immunonegative synaptic terminals (Ter). Note in **b**, an excitatory bouton making synapse with a DAGL-α immunopositive dendrite. **d**, **e** Show in detail the distribution of DAGL-α immunoparticles in dendritic spines (Sp), particularly in the spine neck. Note how spines emerge from their corresponding dendrites that elongate to receive the synaptic contact from the corresponding synaptic terminal. *Scale bars* 0.5 μm. **f** 54.4 ± 3.0 % of dendrites and 44.4 ± 9.4 % of spines are DAGL-α immunopositive ($\chi^2 = 2.220$, $p = 0.1363$) (differences not statistically significant). Numbers between parentheses indicate the number of analyzed profiles. Total analyzed area 1,889 μm^2

NAPE-PLD expressing cells in the VMH (Egertová et al. 2008; Nyilas et al. 2008).

There is certain discrepancy about the localization of NAPE-PLD in different brain regions. Some studies have described a presynaptic localization of NAPE-PLD (Egertová et al. 2008; Nyilas et al. 2008). This distribution of NAPE-PLD in axonal compartments suggests that anandamide and other related *N*-acylethanolamines may be synthesized in presynaptic elements and act as anterograde messengers (Kano et al. 2009).

On the other hand, other studies have shown a postsynaptic localization of NAPE-PLD in some specific neuronal

populations (Cristino et al. 2008; Puente et al. 2011). This may explain a postsynaptic synthesis of anandamide that acts retrogradely activating presynaptic CB_1 receptors and/or postsynaptically modulating synaptic transmission and plasticity through TRPV1 receptors (Chávez et al. 2010; Grueter et al. 2010; Puente et al. 2011). Therefore, in view of the previous studies and our results, the presynaptic and postsynaptic localization of NAPE-PLD in the dorsomedial VMH suggests that anandamide and/or other *N*-acylethanolamines may act as anterograde and/or retrograde messengers in this hypothalamic nucleus.

Ultrastructural localization of DAGL-α in the dorsomedial VMH

We have demonstrated the subcellular localization of DAGL-α in postsynaptic dendritic profiles in the dorsomedial region of the VMH. In general, these results agree with previous studies that described the postsynaptic distribution of DAGL-α in somatodendritic compartments, particularly in dendritic spines of cerebellar Purkinje cells, striatal medium spiny neurons, prefrontal cortical and hippocampal pyramidal neurons, dentate granule cells and neurons in the bed nucleus of the stria terminalis (Katona et al. 2006; Yoshida et al. 2006; Lafourcade et al. 2007; Uchigashima et al. 2007, 2011; Puente et al. 2011).

The density of DAGL-α in the dorsomedial VMH was estimated to be 0.57 particles/μm in dendrites and 1.02 particles/μm in spines. This density is higher than the one described in dendrites and spines of the dentate granule cells (Uchigashima et al. 2011). However, the DAGL-α density in the dorsomedial VMH is much lower than in Purkinje cell dendrites and spines (Yoshida et al. 2006). Therefore, DAGL-α labeling density varies among different subcellular compartments and cell types. This distinct and fine localization of DAGL-α in neuronal types suggests that the specificity and efficiency of the retrograde suppression mediated by endocannabinoids depend not only on the expression levels of CB_1 in the presynaptic elements, but also on the amount of the synthesizing enzyme and the distance between the postsynaptic site of 2-AG production and the presynaptic CB_1 (Yoshida et al. 2006).

Functional significance

In the hypothalamus, the levels of the two main endocannabinoids, anandamide and 2-AG, increase after fasting and decrease after food intake (Kirkham et al. 2002; Di Marzo and Matias 2005; Pagotto et al. 2006; Matias and Di Marzo 2007). Therefore, the presence of the synthesizing enzymes must be upregulated or downregulated depending on the state of hunger or satiety of the animal, which must be synchronized at the same time with the corresponding levels of the degradation enzymes.

Therefore, the precise subsynaptic localization of DAGL-α shown here is a key player that determines available 2-AG levels to reach presynaptic CB_1 receptors distributed at excitatory and inhibitory synapses in the VMH (Reguero et al. 2011). This may facilitate food intake after fasting if a low level of 2-AG acts over CB_1 in excitatory terminals, or reduce food intake if higher levels of 2-AG are available at CB_1 in inhibitory terminals, as shown with low and high doses of exogenous THC, respectively (Bellocchio et al. 2010). Regarding anandamide, more studies are needed to complement the anatomical results obtained here in order to know its role in all these processes of synaptic signaling as well as to understand the mechanisms by which anandamide administration into the VMH stimulates appetite (Jamshidi and Taylor 2001).

Acknowledgments This work has been supported by The Basque Country Government Grant BCG IT764-13; Ministerio de Economía y Competitividad (MINECO) Grant BFU2012-33334; University of the Basque Country UPV/EHU UFI11/41 and Red de Transtornos Adictivos (RTA)—Instituto de Salud Carlos III grant RD12/0028/0004. L. Reguero was supported by a Postdoctoral Specialization Contract from the University of the Basque Country UPV/EHU.

References

Basavarajappa BS (2007) Critical enzymes involved in endocannabinoid metabolism. Protein Pept Lett 14:237–246

Bellocchio L, Lafenêtre P, Cannich A, Cota D, Puente N, Grandes P, Chaouloff F, Piazza PV, Marsicano G (2010) Bimodal control of stimulated food intake by the endocannabinoid system. Nat Neurosci 13:281–283

Berthoud HR (2002) Multiple neural systems controlling food intake and body weight. Neurosci Biobehav Rev 26:393–428

Chávez AE, Chiu CQ, Castillo PE (2010) TRPV1 activation by endogenous anandamide triggers postsynaptic long-term depression in dentate gyrus. Nat Neurosci 13(12):1511–1518

Colombo G, Agabio R, Diaz G, Lobina C, Reali R, Gessa GL (1998) Appetite suppression and weight loss after the cannabinoid antagonist SR 141716. Life Sci 63(8):PL113–PL117

Cota D, Genghini S, Pasquali R, Pagotto U (2003) Antagonizing the cannabinoid receptor type 1: a dual way to fight obesity. J Endocrinol Invest 26(10):1041–1044

Cota D, Woods S (2005) The role of the endocannabinoid system in the regulation of energy homeostasis. Curr Opin Endocrinol Diabetes 12:338–351

Cristino L, Starowicz K, De Petrocellis L, Morishita J, Ueda N, Guglielmotti V, Di Marzo V (2008) Immunohistochemical localization of anabolic and catabolic enzymes for anandamide and other putative endovanilloids in the hippocampus and cerebellar cortex of the mouse brain. Neuroscience 151:955–968

De Petrocellis L, Cascio MG, Di Marzo V (2004) The endocannabinoid system: a general view and latest additions. Br J Pharmacol 141:765–774

Devane WA, Hanus L, Breuer A, Pertwee RG, Stevenson LA, Griffin G, Gibson D, Mandelbaum A, Etinger A, Mechoulam R (1992)

Isolation and structure of a brain constituent that binds to the cannabinoid receptor. Science 258:1946–1949
Di Marzo V, Matias I (2005) Endocannabinoid control of food intake and energy balance. Nat Neurosci 8:585–589
Di Marzo V, De Petrocellis L, Bisogno T (2001) Endocannabinoids Part I: molecular basis of endocannabinoid formation, action and inactivation and development of selective inhibitors. Expert Opin Ther Targets 5(2):241–265
Egertová M, Giang DK, Cravatt BF, Elphick MR (1998) A new perspective on cannabinoid signalling: complementary localization of fatty acid amide hydrolase and the CB1 receptor in rat brain. Proc Biol Sci 265:2081–2085
Egertová M, Cravatt BF, Elphick MR (2003) Comparative analysis of fatty acid amide hydrolase and cb(1) cannabinoid receptor expression in the mouse brain: evidence of a widespread role for fatty acid amide hydrolase in regulation of endocannabinoid signaling. Neuroscience 119:481–496
Egertová M, Simon GM, Cravatt BF, Elphick MR (2008) Localization of N-acyl phosphatidylethanolamine phospholipase D (NAPE-PLD) expression in mouse brain: a new perspective on N-acylethanolamines as neural signaling molecules. J Comp Neurol 506:604–615
Grueter BA, Brasnjo G, Malenka RC (2010) Postsynaptic TRPV1 triggers cell type-specific long-term depression in the nucleus accumbens. Nat Neurosci 13:1519–1525
Gulyas AI, Cravatt BF, Bracey MH, Dinh TP, Piomelli D, Boscia F, Freund TF (2004) Segregation of two endocannabinoid-hydrolyzing enzymes into pre- and postsynaptic compartments in the rat hippocampus, cerebellum and amygdala. Eur J Neurosci 20:441–458
Hegyi Z, Holló K, Kis G, Mackie K, Antal M (2012) Endocannabinoid system in the adult rat circumventricular areas: an immunohistochemical study. Glia 60:1316–1329
Jamshidi N, Taylor DA (2001) Anandamide administration into the ventromedial hypothalamus stimulates appetite in rats. Br J Pharmacol 134:1151–1154
Kano M, Ohno-Shosaku T, Hashimotodani Y, Uchigashima M, Watanabe M (2009) Endocannabinoid-mediated control of synaptic transmission. Physiol Rev 89:309–380
Katona I, Urbán GM, Wallace M, Ledent C, Jung KM, Piomelli D, Mackie K, Freund TF (2006) Molecular composition of the endocannabinoid system at glutamatergic synapses. J Neurosci 26:5628–5637
Kim KW, Jo YH, Zhao L, Stallings NR, Chua SC Jr et al (2008) Steroidogenic factor 1 regulates expression of the cannabinoid receptor 1 in the ventromedial hypothalamic nucleus. Mol Endocrinol 22:1950–1961
Kirkham TC, Williams CM, Fezza F, Di Marzo V (2002) Endocannabinoid levels in rat limbic forebrain and hypothalamus in relation to fasting, feeding and satiation: stimulation of eating by 2-arachidonoyl glycerol. Br J Pharmacol 136:550–557
Lafourcade M, Elezgarai I, Mato S, Bakiri Y, Grandes P, Manzoni OJ (2007) Molecular components and functions of the endocannabinoid system in mouse prefrontal cortex. PLoS ONE 2:e709
Leung D, Saghatelian A, Simon GM, Cravatt BF (2006) Inactivation of N-acyl phosphatidylethanolamine phospholipase D reveals multiple mechanisms for the biosynthesis of endocannabinoids. Biochemistry 45:4720–4726
Matias I, Di Marzo V (2007) Endocannabinoids and the control of energy balance. Trends Endocrinol Metab 18:27–37
McClellan KM, Parker KL, Tobet S (2006) Development of the ventromedial nucleus of the hypothalamus. Front Neuroendocrinol 27:193–209
Mechoulam R, Ben-Shabat S, Hanus L, Ligumsky M, Kaminski NE, Schatz AR, Gopher A, Almog S, Martin BR, Compton DR, Pertwee RG, Griffin G, Bayewitch M, Barg J, Vogel Z (1995) Identification of an endogenous 2-monoglyceride, present in canine gut, that binds to cannabinoid receptors. Biochem Pharmacol 50:83–90
Morishita J, Okamoto Y, Tsuboi K, Ueno M, Sakamoto H, Maekawa N, Ueda N (2005) Regional distribution and age-dependent expression of N-acylphosphatidylethanolamine-hydrolyzing phospholipase D in rat brain. J Neurochem 94:753–762
Nyilas R, Dudok B, Urbán GM, Mackie K, Watanabe M, Cravatt BF, Freund TF, Katona I (2008) Enzymatic machinery for endocannabinoid biosynthesis associated with calcium stores in glutamatergic axon terminals. J Neurosci 28:1058–1063
Pagotto U, Marsicano G, Cota D, Lutz B, Pasquali R (2006) The emerging role of the endocannabinoid system in endocrine regulation and energy balance. Endocr Rev 27:73–100
Puente N, Cui Y, Lassalle O, Lafourcade M, Georges F, Venance L, Grandes P, Manzoni OJ (2011) Polymodal activation of the endocannabinoid system in the extended amygdala. Nat Neurosci 14:1542–1547
Reguero L, Puente N, Elezgarai I, Mendizabal-Zubiaga J, Canduela MJ, Buceta I, Ramos A, Suárez J, de Fonseca FR, Marsicano G, Grandes P (2011) GABAergic and cortical and subcortical glutamatergic axon terminals contain CB1 cannabinoid receptors in the ventromedial nucleus of the hypothalamus. PLoS ONE 6:e26167
Sternson SM, Shepherd GM, Friedman JM (2005) Topographic mapping of VMH –> arcuate nucleus microcircuits and their reorganization by fasting. Nat Neurosci 8(10):1356–1363
Suárez J, Romero-Zerbo SY, Rivera P, Bermúdez-Silva FJ, Pérez J, De Fonseca FR, Fernández-Llebrez P (2010) Endocannabinoid system in the adult rat circumventricular areas: an immunohistochemical study. J Comp Neurol 518:3065–3085
Sugiura T, Kondo S, Sukagawa A, Nakane S, Shinoda A, Itoh K, Yamashita A, Waku K (1995) 2-Arachidonoyl-glycerol: a possible endogenous cannabinoid receptor ligand in brain. Biochem Biophys Res Commun 215:89–97
Tanimura A, Yamazaki M, Hashimotodani Y, Uchigashima M, Kawata S, Abe M, Kita Y, Hashimoto K, Shimizu T, Watanabe M, Sakimura K, Kano M (2010) The endocannabinoid 2-arachidonoylglycerol produced by diacylglycerol lipase alpha mediates retrograde suppression of synaptic transmission. Neuron 65:320–327
Tanimura A, Uchigashima M, Yamazaki M, Uesaka N, Mikuni T, Abe M, Hashimoto K, Watanabe M, Sakimura K, Kano M (2012) Synapse type-independent degradation of the endocannabinoid 2-arachidonoylglycerol after retrograde synaptic suppression. Proc Natl Acad Sci USA 109:12195–12200
Uchigashima M, Narushima M, Fukaya M, Katona I, Kano M, Watanabe M (2007) Subcellular arrangement of molecules for 2-arachidonoyl-glycerol-mediated retrograde signaling and its physiological contribution to synaptic modulation in the striatum. J Neurosci 27:3663–3676
Uchigashima M, Yamazaki M, Yamasaki M, Tanimura A, Sakimura K, Kano M, Watanabe M (2011) Molecular and morphological configuration for 2-arachidonoylglycerol-mediated retrograde signaling at mossy cell-granule cell synapses in the dentate gyrus. J Neurosci 31:7700–7714
Yoshida T, Fukaya M, Uchigashima M, Miura E, Kamiya H, Kano M, Watanabe M (2006) Localization of diacylglycerol lipase-alpha around postsynaptic spine suggests close proximity between production site of an endocannabinoid, 2-arachidonoyl-glycerol, and presynaptic cannabinoid CB1 receptor. J Neurosci 26:4740–4751
Yoshida T, Uchigashima M, Yamasaki M, Katona I, Yamazaki M, Sakimura K, Kano M, Yoshioka M, Watanabe M (2011) Unique inhibitory synapse with particularly rich endocannabinoid signaling machinery on pyramidal neurons in basal amygdaloid nucleus. Proc Natl Acad Sci USA 108:3059–3064